

Detection of epileptic seizure in EEG signals using linear least squares preprocessing

Z. Roshan Zamir^{a,*}

^a*Faculty of Science, Engineering and Technology, Swinburne University of Technology,
PO Box 218, Hawthorn, Victoria, Australia*

Abstract

An epileptic seizure is a transient event of abnormal excessive neuronal discharge in the brain. This unwanted event can be obstructed by detection of electrical changes in the brain that happen before the seizure takes place. The automatic detection of seizures is necessary since the visual screening of EEG recordings is a time consuming task and requires experts to improve the diagnosis. Four linear least squares-based preprocessing models are proposed to extract key features of an EEG signal in order to detect seizures. The first two models are newly developed. The original signal (EEG) is approximated by a sinusoidal curve. Its amplitude is formed by a polynomial function and compared with the pre developed spline function. Different statistical measures namely classification accuracy, true positive and negative rates, false positive and negative rates and precision are utilized to assess the performance of the proposed models. These metrics are derived from confusion matrices obtained from classifiers. Different classifiers are used over the original dataset and the set of extracted features. The proposed models significantly reduce the dimension of the classification problem and the computational time while the classification accuracy is improved in most cases. The first and third models are promising feature extraction methods. Logistic, LazyIB1, LazyIB5 and J48 are the best classifiers. Their true positive and negative rates are 1 while false positive and negative rates are zero and the corresponding precision values are 1. Numerical results suggest that these models are robust and efficient for detecting epileptic seizure.

*Corresponding author

Email address: roshanzamir.zahra@gmail.com (Z. Roshan Zamir)

Keywords: Biological signal classification, Signal approximation, Feature extraction, Data analysis, Linear least squares problems, EEG Seizure detection

2010 MSC: 92C55, 65D15, 65D07, 65K05, 90C25

1. Introduction

An *electroencephalogram* (EEG) is an electrical activity of the human brain that can be recorded graphically. Electrical activity is generated by firing of neurones of the human brain due to internal or external stimuli to control different bodily actions. Epilepsy is a neurological disorder disease that manifests in about one percentage of the world's population [1]. It is characterized by a recurrent seizure that happens when the neurons generate abnormal electrical discharges from brain cells. A seizure is experienced in about 5% of individuals in their life [2] and approximately 30% of patients have disobedient seizure that can lead to the neural tissues disorders [3]. The seizure can be treated by medication in 70% of patients [4].

The seizure can cause physical changes in behavior and movements, loss of consciousness, muscle spasms, strange emotions and even death. Therefore, detection of epilepsy is still a challenging issue for medical diagnosis of epilepsy. An EEG is a well known tool for identification of epileptic seizure since it measures the voltage fluctuations of the brain [5, 6] and provides important information about epileptic activities. Visual detection of epileptic seizure in an EEG signal is being time consuming and causing fatigue and requires highly trained practitioners. Different steps like preprocessing, features extraction and classification can be involved in an epileptic seizure detection technique.

There have been various attempts for automatic detection of epilepsy based on Wavelet Transforms [7, 8, 9], Artificial Neural Networks [10, 11] and Genetic Programming [12]. Panda *et al.*, 2010 [13] applied discrete wavelet transform and a classifier called support vector machine (SVM) to compute various features like energy, entropy and standard deviation. They obtained the classification accuracy of 91.2%. The classification accuracy of 96.7% was obtained through mixed-band wavelet chaos neural network method by Dastidar *et al.*, 2007 [14]. They used wavelet transformation to break up the EEG signals into different range of frequencies and three features namely standard deviation, correlation dimension and the largest Lyapunov exponent

were used and different methods employed for classification. To decompose the normal and epileptic EEG epochs to various frequency bands and to find optimal features subsets which maximize the classification performance, fourth level wavelet packet decomposition method was proposed by Ocak [15]. The classification accuracy of this method was 98%. Polat *et al.*, (2007) [16] applied two stage processes. First one was First Fourier Transform (FFT) as a feature extractor and second one was decision making classifier. They got a classification accuracy of 98.72%. Bhardwaj *et al.*, 2015 [12] applied an automated detection of epileptic seizures in EEG signals using Empirical Mode Decomposition (EMD) for feature extraction and proposed a Constructive Genetic Programming (CGP) approach for classifying the EEG signals. The classification accuracies of 100% and 99.41% (an average classification accuracy) were obtained from one Genetic Programming (GP) run and 100 GP runs respectively through a CGP for 10-fold cross validation scheme. A new method for classification of ictal and seizure-free EEG signals was presented by Pachori and Patidar in 2014 [17]. The proposed method was based on the EMD and Second-order Difference Plot (SODP) of Intrinsic Mode Functions (IMFs). They computed the 95% confidence ellipse area parameters for ictal and seizure-free classes using SODP of IMFs for various window sizes. The best average classification accuracy of 97.75% was obtained for IMF1 and IMF2 with window size of 1000. The maximum classification accuracy was 100%. To the best of our knowledge, the best method in terms of classification accuracy was developed by Bajaj *et al.*, 2012 [18]. For the classification of seizure and non-seizure EEG signals they applied least square SVM (LS-SVM) and they got the classification accuracies of 98% to 99.5% using radial basis function (RBF) kernel and 99.5% to 100% using Morlet kernel.

A considerably amount of literature has been reported the accuracy as the criterion to assess their performances. The evidence from this study shows that this criterion is based on the proportion of correctly and incorrectly classified segments. It is worth to mention that the above techniques used the Bonn University dataset [19]. High classification accuracies may be acquired owing to the existence of unbalanced datasets where a disproportionately large amount of segments (instances) belongs to a certain class although the proposed classifier may not necessarily be good. As an alternative to classification accuracy, the area under the Receiver Operating Characteristic (ROC) curve can be used to assess the classification accuracy where there exist unbalanced datasets [20]. The ROC curve is produced by plotting the fraction of True Positive Rate (TPR) against the fraction of False Positive Rate (FPR)

as the threshold for discrimination between two classes is varied [20]. The definitions of TPR and FPR are provided in Section 3.2. None of the previous techniques explored the consistency in performances. More research should be conducted to detect epileptic seizure by analysing EEG signals since it is a challenging task due to inconsistency of signals in patient's sex, seizure's type, patient's age and so on. To address this issue, the dataset described in [19] is balanced and used to validate the proposed method of identifying epileptic seizure.

One of the main characteristics of epileptic seizure is excessive increases in signal amplitude. Continuous piecewise polynomials that are known as splines are flexible and suited candidates to model abrupt changes in amplitude [21, 22]. In addition, it is illustrated in [21, 22] that the simpler modelling functions are very efficient and work well. Therefore, these facts motivate the author to model the brain signal as sinusoidal waves with

- spline and
- polynomial (that is simpler than spline)

amplitudes. These enable one to

- develop an accurate model for the wave shapes and
- extract key features of the waves that are crucial for detecting seizures.

These features are extracted through minimizing the sum of the squares of the deviation between the original signal and the modelling functions. However, this approach leads to the necessity of solving a sequence of linear least squares problems that is a subclass of convex optimisation problems. After extracting the features, classification algorithms (classifiers) are applied over the set of extracted features to evaluate the classification accuracy of an EEG signal in presence of seizures.

This paper proposes a novel method based on two Linear Least Squares-based Preprocessing models (LLSPs) and different classifiers from WEKA [23] for automatic detection of an epileptic seizure in EEG signals.

This work is aimed at discovering the optimal approximation of an EEG signal under a sinusoidal modelling function and consistency improving the performance of LLSPs in classification problems compared with the original signal. Employing LLSPs as preprocessing-based models lead to dimension reduction and essential features extraction of an EEG signal. One interesting

finding is that if the extracted features from a signal are not accurate enough to describe the original signal, the classification algorithms will not recognize those features appropriately. So, in order to improve the performance of classification algorithms, extracting good features via proposed method is essential. Many researchers have reported that a sophisticated adjustment through proper analysis methods can significantly enhance the classification accuracy [24]. It should be noted that providing a good trade off between a high classification accuracy and a low false positive rate (FPR) is a difficult problem in classification purposes.

The rest of this paper is structured as follows. Section 2 presents new developed models for seizure detection based on the LLSP to extract key features of a signal. Section 3 presents the numerical experiments and analyses the outcomes. Section 4 provides the final remarks.

2. Methods

2.1. Linear least squares-based preprocessing

The LLSPs have been well studied in signal approximation [21, 22, 25].

- First in [21], authors approximated an EEG signal by a sine wave with a piecewise polynomial function as an amplitude to detect the K-complexes in an EEG background. The corresponding frequencies and shifts were constants and formed a fine grid. They needed to optimise parameters of the amplitude for each combination of frequency and shift values on the fine grid. Therefore, a sequence of linear least squares problems were developed and solved. The authors reported that this approach is much faster than the one in [26] and the corresponding classification accuracy is high. Unlike the approach developed in [21] ω and τ were modelled as additional variables in [26] .
- Second, in [22], authors developed another three convex optimisation-based models for automatic detection of K-complexes. The first model was similar to that one in [21] where the wave was oscillating around zero. The second model was developed differently such that the wave defined in the first model was shifted vertically by a spline (piecewise polynomial) function. In conclusion, the new developed models were robust, efficient, fast and accurate due to the fact that they are simple, smooth, linear and inexpensive.

The splines are more desirable if the locations of their knots are optimised. Challenging this issue, one might need to work with free knots instead of fixed ones. In this case, the problem becomes non-convex that is computationally expensive and non-smooth. An alternative to non-convex reformulation is to avoid non-convexity from the beginning by modelling a signal amplitude as a spline function with higher dimension fixed knots (more subintervals) rather than a free knots one [21, 22].

There are some strategies for the optimal knots localization [27, 28] for those who do not like this simplifying [29]. The efficiency of simpler modelling functions was demonstrated in [21, 22] therefore, two new feature extraction models based on polynomials are developed such that a polynomial of increased degree is employed where there are no interval divisions.

The main contributions of this work are as follows.

- To develop approximation models that are
 - categorized under convex and smooth optimisation problems;
 - simple and computationally inexpensive;
 - accurate enough to extract essential characteristics of an EEG signal and provide a high level of accuracy while achieving a low FPR.
- To execute the proposed models on epileptic EEG signals and compare them based on different statistical measures like Classification Accuracy (ACC), TPR, True Negative Rate (TNR), FPR, False Negative Rate (FNR) and corresponding computational time.

The definitions of ACC, TPR, TNR, FPR and FNR are provided in Section 3.2

2.2. Signal amplitudes

Capturing extended amplitude changes is a reasonable approach to detect epilepsy. To approximate the amplitude of an EEG signal one possibility is through the spline functions [21, 22] and another possibility is to use the polynomial ones. Spline functions are naturally suitable candidates to describe a polynomial-like behavior of a signal. They are flexible to abrupt changes. In these functions one can switch from one polynomial to another

and the switch points called knots. There are many ways to construct spline functions. The most common one is based on a truncated power function [30].

$$S_m(\mathbf{x}, \boldsymbol{\theta}, t) = x_0 + \sum_{j=1}^m x_{1j} t^j + \sum_{l=2}^n \sum_{j=1}^m x_{lj} (t - \theta_{l-1})_+^j, \quad (1)$$

where $\mathbf{x} = [x_0, x_{11}, \dots, x_{nm}]$ are the spline parameters, m is the degree of a spline, n is the number of subintervals in a D seconds duration of an EEG signal, t is a T seconds duration of each subinterval, $\boldsymbol{\theta} = (\theta_1, \dots, \theta_{n-1})$ are the equidistant fixed knots and

$$(t - \theta_{l-1})_+ = \max\{0, (t - \theta_{l-1})\}, \quad (2)$$

is the truncated power function. Since simple models are fast and accurate enough to approximate a signal the amplitude is approximated as a polynomial function instead of spline one. The polynomial functions may not be as flexible as spline ones, but they are simpler and fast. The polynomial is modelled as an amplitude function when the number of subintervals in Equation (1) is selected to be 1 ($n = 1$). Therefore,

$$P_m(\mathbf{x}, t) = x_0 + \sum_{j=1}^m x_j t^j, \quad (3)$$

To determine the signal amplitude approximated by a spline (1) and polynomial (3) functions, their parameters should be specified. To address this, LLSPs are employed.

2.3. Feature extraction models

Feature extraction techniques play an important role in identifying the main characteristics of a signal (extract information from data), reducing the dimensionality of data and classification of a signal. In this section, four feature extraction models are supposed. The first two models are newly developed while the last two ones were developed in [21, 22]. Their performances and effectivenesses in terms of classification of an EEG signal in presence of seizures will be investigated subsequently.

2.3.1. Linear Least Squares-based Preprocessing 1 (LLSP1)

This new model is formulated in such a way that the amplitude is approximated as a polynomial function described in (3). The wave is modelled as

$$W_1 = \text{Amp}_{m,1}(\mathbf{x}, t_i) \sin(\omega t_i + \tau), \quad (4)$$

where $\text{Amp}_{m,1}$ is the polynomial function P_m defined in (3), m is the degree of a polynomial, $\mathbf{x} = [x_0, x_1, \dots, x_m] \in \mathbb{R}^{m+1}$, $t_i \in \mathbb{R}^N$ for $i = 1, \dots, N$ (N is the total number of signal recordings), ω is the frequency and τ is the phase (shift). If a frequency modulation is considered in this signal approximation, the problem becomes non-convex. Therefore, the explicit optimisation of frequencies is very complex problem that also known as Mandelsham's problem [31, 32]. Consequently, the signal amplitude modulations are presented in this work. The range of possible frequencies and shifts form a fine grid. Hence, for each combination of ω and τ values on the fine grid the LLSP1 is

$$\min_{\mathbf{x}} \sum_{i=1}^N (y_i - W_1)^2. \quad (5)$$

Equation (5) is rewritten as

$$\min_{\mathbf{x}} \sum_{i=1}^N (y_i - (M_1 \mathbf{x})_i)^2, \quad \text{or} \quad \min_{\mathbf{x}} \|M_1 \mathbf{x} - \mathbf{y}\|_2^2, \quad (6)$$

where y_i , $i = 1, \dots, N$ are the recorded signals at $t_i \in \mathbb{R}^N$, $\mathbf{x} \in \mathbb{R}^{m+1}$, $\mathbf{y} = (y_1, y_2, \dots, y_N)^T \in \mathbb{R}^N$, $(M_1 \mathbf{x})_i$ is the i -th component of the vector $M_1 \mathbf{x}$ and M_1 is a matrix with $m + 1$ columns and N rows of the form $\text{Amp}_{m,1}(t_i) \sin(\omega t_i + \tau)$. Matrix M_1 is a full-rank matrix [25]. Therefore, the unique solution to this problem can be obtained by solving the following normal equations

$$(M_1^T M_1) \mathbf{x} = M_1^T \mathbf{y}, \quad (7)$$

and its analytical solution is

$$\mathbf{x} = (M_1^T M_1)^{-1} M_1^T \mathbf{y}, \quad (8)$$

where $\mathbf{y} = (y_1, \dots, y_N)^T \in \mathbb{R}^N$ are signal segments recorded at N distinct consecutive time moments. Matrix M_1 is detailed below.

$$M_1^{N \times (m+1)} = \begin{bmatrix} \alpha_1 & \alpha_1 t_1 & \dots & \alpha_1 t_1^m \\ \alpha_2 & \alpha_2 t_2 & \dots & \alpha_2 t_2^m \\ \vdots & \vdots & \ddots & \vdots \\ \alpha_N & \alpha_N t_N & \dots & \alpha_N t_N^m \end{bmatrix}, \quad (9)$$

where $\alpha_i = \sin(\omega t_i + \tau)$.

2.3.2. Linear Least Squares-based Preprocessing 2 (LLSP2)

This new model is formulated differently from the way it is formulated in LLSP1. Here, the wave described in (4) is shifted vertically by a polynomial function with the same degree defined in (3).

$$W_2 = Amp_{m,1}(\mathbf{x}_1, t_i) \sin(\omega t_i + \tau) + Amp_{m,1}(\mathbf{x}_2, t_i), \quad (10)$$

hence, the LLSP2 is

$$\min_{\mathbf{x}} \sum_{i=1}^N (y_i - W_2)^2, \quad (11)$$

where $\mathbf{x} = [\mathbf{x}_1; \mathbf{x}_2] \in \mathbb{R}^{2m+2}$ are the polynomial parameters. The dimension of this problem is $2m + 2$ while the dimension of LLSP1 is $m + 1$. Equation (11) is rewritten as

$$\min_{\mathbf{x}} \sum_{i=1}^N (y_i - (B_1 \mathbf{x})_i)^2, \quad \text{or} \quad \min_{\mathbf{x}} \|B_1 \mathbf{x} - \mathbf{y}\|_2^2, \quad (12)$$

where $\mathbf{y} = (y_1, \dots, y_N)^T \in \mathbb{R}^N$, $\mathbf{x} = [\mathbf{x}_1; \mathbf{x}_2] \in \mathbb{R}^{2m+2}$ are the polynomial parameters and matrix B_1 contains $2m + 2$ columns and N rows of the form $Amp_{m,1}(t_i) \sin(\omega t_i + \tau) + Amp_{m,1}(t_i)$ and is made up of the following matrices:

$$B_1^{N \times (2m+2)} = [M_1^{N \times (m+1)} \quad B_2^{N \times (m+1)}],$$

where M_1 is defined in (9) and B_2 is

$$B_2^{N \times (m+1)} = \begin{bmatrix} 1 & t_1 & \dots & t_1^m \\ 1 & t_2 & \dots & t_2^m \\ \vdots & \vdots & \ddots & \vdots \\ 1 & t_N & \dots & t_N^m \end{bmatrix}. \quad (13)$$

Matrix B_1 is a rank-deficient matrix and $B_1^T B_1$ is a singular matrix. The singularity study of this matrix is provided in [25]. Therefore, the system of normal equations has no unique solution to LLSP2 then, to address this issue a Singular Value Decomposition (SVD) is applied for solving this problem.

2.3.3. Linear Least Squares-based Preprocessing 3 (LLSP3)

An EEG signal is modelled as a sine wave such that

$$W_3 = Amp_{m,n}(\mathbf{x}, \boldsymbol{\theta}, t_i) \sin(\omega t_i + \tau), \quad (14)$$

where $Amp_{m,n}$ is the spline function S_m defined in (1) whose $\boldsymbol{\theta} = (\theta_1, \dots, \theta_{n-1})$ are fixed (equidistant), ω is the frequency and τ is the phase (shift). The range of possible frequencies and shifts form a fine grid. Therefore, for each combination of ω and τ values on the fine grid the LLSP3 is

$$\min_{\mathbf{x}} \sum_{i=1}^N (y_i - W_3)^2, \quad (15)$$

where y_i , $i = 1, \dots, N$ are the EEG recordings at the moment t_i . Equation (15) is rewritten as

$$\min_{\mathbf{x}} \sum_{i=1}^N (y_i - (M\mathbf{x})_i)^2, \quad \text{or} \quad \min_{\mathbf{x}} \|M\mathbf{x} - \mathbf{y}\|_2^2, \quad (16)$$

where $(M\mathbf{x})_i$ is the i -th component of the vector $M\mathbf{x}$, vector $\mathbf{x} \in \mathbb{R}^{mn+1}$, $\mathbf{y} = (y_1, y_2, \dots, y_N)^T \in \mathbb{R}^N$ and M is a matrix with N rows of the form $Amp_{m,n}(\boldsymbol{\theta}, t_i) \sin(\omega t_i + \tau)$ and $mn + 1$ columns. If $M \in \mathbb{R}^{N \times (mn+1)}$ is a full-rank matrix, then, least squares solution can be found by solving the normal equations [33]

$$(M^T M)\mathbf{x} = M^T \mathbf{y}, \quad (17)$$

directly and its analytical solution is

$$\mathbf{x} = (M^T M)^{-1} M^T \mathbf{y}. \quad (18)$$

In this case, matrix M is a full rank matrix [25] and matrix $M^T M$ is known to be nonsingular and well-conditioned [34] therefore, the solution of the normal equations is unique.

2.3.4. Linear Least Squares-based Preprocessing 4 (LLSP4)

In this model, the wave described in (14) is shifted vertically by a spline function such that

$$W_4 = Amp_{m,n}(\mathbf{x}_1, \boldsymbol{\theta}, t_i) \sin(\omega t_i + \tau) + Amp_{m,n}(\mathbf{x}_2, \boldsymbol{\theta}, t_i), \quad (19)$$

so, the corresponding preprocessing problem is

$$\min_{\mathbf{x}} \sum_{i=1}^N (y_i - W_4)^2, \quad (20)$$

where y_i are signal recordings at t_i for $i = 1, 2, \dots, N$ and $\mathbf{x} = [\mathbf{x}_1; \mathbf{x}_2]$ are the spline parameters. The vertical shift is modelled as another spline function with the same degree and knots defined in (1). The dimension of this problem is $2mn + 2$ while the dimension of LLSP3 is $mn + 1$. LLSP4 in (20) is reformulated as

$$\min_{\mathbf{x}} \sum_{i=1}^N (y_i - (B\mathbf{x})_i)^2, \quad \text{or} \quad \min_{\mathbf{x}} \|B\mathbf{x} - \mathbf{y}\|_2^2. \quad (21)$$

$Amp_{m,n}(\boldsymbol{\theta}, t_i) \sin(\omega t_i + \tau) + Amp_{m,n}(\boldsymbol{\theta}, t_i)$ is the form of N rows of matrix B . Further, matrix B contains $2mn + 2$ columns. It is illustrated in [22] that B is a rank-deficient matrix and therefore, $B^T B$ is a singular matrix. Sufficient conditions of nonsingularity of matrix B is provided in [25]. An SVD is more robust and reliable than normal equations for solving rank-deficient problems [35, 33, 36]. So, an SVD is employed to solve LLSP4 defined in (20) [22]. Figure (1) shows the flowchart of LLSPs (the LLSP1 to LLSP4).

Figure 1. LLSP approaches Flowchart.

2.4. Classification of an EEG signal

The LLSPs reduce the size of classification problem and extract the essential features of an EEG signal. Key features contains the optimal values of objective function, ω , τ and amplitude parameters for each segment. The classification accuracy of an EEG signal for detecting an epileptic seizure is obtained by employing the classification algorithms from WEKA [23] on the original dataset and preprocessed dataset after LLSPs. WEKA is an open source data analysis software, its web-site [23] provides all the necessary documentation therefore, we only provide a very short description of the classifiers used in this study. Following 12 classification algorithms (classifiers) are evaluated.

- LibSVM - an integrated software for support vector machines (SVM) classification [23];
- Logistic - a generalized linear model used for binomial regression [23];
- RBF - a classifier that implements a normalized Gaussian radial basis function network, using the K-means clustering algorithm to provide the basis functions [23];
- SMO - a sequential minimal optimisation algorithm for training a support vector classifier (a special case of LibSVM) [23];
- Lazy IBK - a K-nearest neighbors classifier (uses normalized Euclidean distance to find the training instance closest to the given test instance, and predicts the same class as this training instance) [23];
- KStar - an instance-based classifier [23];
- LWL - a locally weighted learning classifier that uses an instance based algorithm to assign instance weights [23];
- OneR - a classifier that uses the minimum error attribute for prediction, discretizing numeric attributes [23];
- J48 and J48graft - a classifier based on C4.5 decision tree [23];
- LMT - a logistic model tree based approach, with logistic regression functions at the leaves [23].

All above classifiers were used with their default sets of parameters, except LazyIBK, which was used with $K = 1$ and 5 .

2.5. Result interpretation and demonstration

For better understanding of how the proposed methods work, the result interpretation is very demanding here. Figure 2 reveals an approximation signal that is generated by W_3 defined in (14) through LLSP3. The original signal contains 200 segments each containing 1000 recordings (features) with a sampling frequency of 173.61 Hz. The frequency grid was specified as the numbers between 0.53 Hz and 40 Hz with the step size of 1 Hz. This signal contains five datasets. More details about datasets are provided in Section 3.1.

Figure 2. Approximation curve after LLSP3.

By using feature extraction methods (LLSPs) one can see the transition from "sequences of recordings" to "sequences of spline parameters and frequencies". Thereafter, WEKA methods were employed to do classification on both aforementioned sequences before and after preprocessing respectively. Since a 1-Nearest neighbors is one of the simplest classifiers, Lazy IB1 is considered as an example of classification method here. This classifier is based on assigning new observations to the classes with the nearest representative from the training set. If the nearest point (from the training set) is from first class the new observation is assigned to first class otherwise second class. Therefore, the improvement of classification accuracy after preprocessing means that the representation of the point (observation) by the corresponding "sequences of spline parameters and frequencies" is better (from classification point of view) than the actual "sequences of recordings". In addition, it means that the approximated signal captures the essential patterns of the original signal accurately.

3. Numerical Experiments

3.1. Data acquisition

The EEG dataset used for this study is collected from the epileptic center at the University of Bonn, Germany and studied by Andrzejak et al. [19]. This dataset is publicly available and employed to validate the proposed methods. It contains five datasets namely A, B, C, D, and E, each containing 100 signal channel EEG segments recorded during 23.6 seconds with a sampling frequency of 173.61 Hz using 12-bit resolution. Band-pass filter settings were 0.53 – 40 Hz (12 dB/oct) therefore, each signal has 4097 recordings (a length of 4097 samples).

Segments belong to sets A and B are collected from surface EEG recordings of five healthy volunteers with eyes open and close respectively. Sets C, D and E were obtained from the presurgical diagnosis of five different epileptic patients. EEG recordings of sets C and D were collected during seizure free intervals while set E includes EEG signals during seizure activity. Recordings of A-B,C-D and E datasets were defined as normal, interictal and ictal signals respectively.

Although many preprocessing approaches were tested on sets A and E and achieved high classification accuracy, the effectiveness of different groups of

datasets was not investigated thoroughly. It is more desirable to investigate the ability of proposed methods to deal with EEG signals containing different combinations of datasets (A,B,C,D and E). To address this issue, four different binary classification problems are made from aforementioned datasets. All experiments described below are aimed at the detection of epileptic seizure.

- Experiment 1: Classification of sets A,B,C,D against set E.

The EEG recordings classified into two different classes. Sets A to D contain non-seizure class and set E contains seizure class.

- Experiment 2: Classification of sets A,C,D against set E.

Sets A,C and D belong to non-seizure class and set E belongs to seizure class. The goal of this experiment is to classify samples of seizure and non-seizure excluding healthy with eyes close.

- Experiment 3: Classification of set B against set E.

Set B is treated as non-seizure class while set E as seizure class.

- Experiment 4: Classification of set A against set E.

Set A belongs to non-seizure class and set E belongs to seizure class.

As mentioned earlier, proper balancing of datasets where there exists the equal number of segments for each class is necessary to avoid inconsistency in EEG signals and improve the performance of classification algorithms. Table 1 describes the datasets belong to the corresponding experiments concisely.

Table 1. Description of the datasets belongs to the experiments.

EEG recordings have five datasets (A, B, C, D and E) each containing 100 segments. They are divided into two classes called non-seizure and seizure for each experiment. In order to balance the datasets, 100 segments (observations) are assigned to each class. These 100 segments are selected as follows.

- Experiment 1: Set E belongs to seizure class and contains 100 segments therefore, the non-seizure class should have 100 segments such that sets A, B, C and D have 25 segments each. Figure 3 shows how these 25 segments are selected. As it can be seen the last 100 segments are selected for the seizure class containing set E.

Figure 3. Segments selection of Experiment 1 for datasets balancing.

- Experiment 2: Similar to Experiment 1, the last 100 segments are selected for the seizure class (set E). Therefore, the non-seizure class should have 100 segments such that sets A, C and D have 33, 33 and 34 segments respectively. Figure 4 illustrates the way these segments are selected.

Figure 4. Segments selection of Experiment 2 for datasets balancing.

- Experiment 3: The second and the last 100 segments are selected for non-seizure (set B) and seizure (set E) classes respectively.
- Experiment 4: The first and the last 100 segments are selected for non-seizure (set A) and seizure (set E) classes respectively.

3.2. Evaluation criteria

To assess the performance of the proposed methods, different statistical measures such as the ACC, TPR, Precision, TNR, FPR and FNR are used. They can be derived from a confusion matrix (CM) that is detailed below.

$$\begin{array}{cc}
 & \begin{array}{cc} \text{Non-seizure} & \text{Seizure} \end{array} \\
 \begin{array}{c} \text{Non-seizure} \\ \text{Seizure} \end{array} & \left[\begin{array}{cc} a & b \\ c & d \end{array} \right].
 \end{array}$$

The aforementioned metrics are described as follows:

1. $\text{ACC} = (a + d) / (a + b + c + d)$ corresponds to the proportion of correctly classified segments against the total number of tested segments.
2. $\text{TPR} = a / (a + b)$ corresponds to the proportion of non-seizure healthy volunteers that have been predicted correctly. This metric is also referred to the Recall value.
3. $\text{Precision} = a / (a + c)$ corresponds to the proportion of the healthy non-seizure volunteers that are truly classified divided by the total number of volunteers classified as non-seizure.
4. $\text{TNR} = d / (c + d)$ measures the rate of seizure patients predicted correctly.
5. $\text{FPR} = b / (a + b)$ belongs to the rate of non-seizure healthy volunteers being categorized as seizure patients.
6. $\text{FNR} = c / (c + d)$ belongs to the rate of seizure patients being categorized as non-seizure healthy volunteers.

3.3. Parameters of classification problem

Each dataset is partitioned into training and test sets. 90% of the dataset is selected as a training set and the rest 10% is for test set. Therefore, all experiments except the first one that are introduced in Section 3.1 has 180 and 20 segments for training and test sets respectively. Further, the Experiment 1 has 178 and 22 segments for training and test sets respectively. So, each of 12 classifiers from WEKA was trained on the training set and tested on the test set and the classification accuracy on the test set is reported. Before applying LLSPs as feature extraction methods the classification problem has 200 segments and 4097 features (attributes). Feature extraction methods significantly reduce the dimension of the problem. Therefore, after applying LLSP1, LLSP3 and LLSP2, LLSP4, the approximated EEG signal has 52 and 101 features respectively with 200 segments.

3.4. Numerical results and discussion

LLSP1–4 were modelled as preprocessing approaches to extract the key features of an EEG signal in order to classify its recordings in presence of epileptic seizures. Because M_1 and M are full-rank matrices then, the normal equations method was employed to solve LLSP1 and LLSP3 whereas an SVD was used to solve LLSP2 and LLSP4 since B_1 and B are full-rank matrices. All preprocessing approaches are carried out in MATLAB R2012b and run on a PC with 3.10 GHz CPU and 8 GB of memory. The classification algorithms implemented in WEKA were used over the obtained set of features after preprocessing approaches.

According to the technical specification of EEG datasets [19], $m = 4$ and $n = 12$ were assigned to the spline function S_m defined in Equation (1). The knots are chosen as a sequence of equidistant knots. The frequency grid was specified as the numbers between $\omega_i = 0.53$ Hz and $\omega_f = 40$ Hz with the step size of 1 Hz based on the given band-pass filter settings (0.53 – 40 Hz (12 dB/oct)) while the initial and final values of $\tau_i = 0$ and $\tau_f = \pi$ with the step size of $\pi/4$ were assigned to the shift (phase) grid.

Output dimensions of LLSP3 and LLSP4 are $mn + 1 = 49$ and $2mn + 2 = 98$ respectively. The polynomial function P_m defined in (3) was modelled as a signal amplitude. In order to balance the number of parameters in spline and polynomial functions, the degree of P_m was increased to 48. So, $m = 48$ was assigned to P_m . Herein, the results from LLSP1 and LLSP2 are comparable with LLSP3 and LLSP4. Output dimensions of LLSP1 and LLSP2 are $m + 1 = 49$ and $2m + 2 = 98$ respectively. Three extra parameters

after an LLSP are considered that are the values of objective function, ω and τ for each segment. Therefore, $N = 4097$ features (recordings) of original dataset have been reduced to 52 and 101 features after LLSP1, LLSP3 and LLSP2, LLSP4 respectively.

Tables 2 and 3 demonstrate the numerical results for LLSPs. Table 2 indicates that LLSP2 and LLSP4 have higher CPU times than LLSP1 and LLSP3. The execution time of LLSP3 is less than LLSP1 therefore, a pre-processing approach with a spline amplitude would be preferable in terms of computational time. LLSP3 had spent the least time to extract the essential features of a signal described in Experiment 1. Table 3 displays the mean frequencies for each set of the EEG signal. One can see that the mean frequencies of seizures (set E) are significantly higher than non-seizures (sets A, B, C and D) except for set B. It may be due to the fact that seizures were identified by the presence of high frequencies activity.

Table 2. Computational time (in seconds) for preprocessing.

Table 3. Mean frequencies for each set of the EEG signal.

First, the classifiers were employed over the original dataset with $N = 4097$ features. The results are shown in the first column of Tables 4, 8, 12, and 16. The "Logistic", "SMO" and "LMT" algorithms do not produce any results on original dataset. This is most probably due to the memory limitations of the used software implementation. Second, all classifiers were applied over the obtained set of features after LLSP approaches. The classification accuracy results based on the four experiments are presented in the Tables 4, 8, 12, and 16.

Because of the long computational time taken for LLSP4 (in Table 2) and the fact that "RBF Network" algorithm in Table 4 provides a better accuracy on the original dataset rather than the preprocessed dataset after LLSP4, the performance of LLSP4 is not satisfactory. Although LLSP2 has a long computational time similar to LLSP4, "RBF Network" and "LibSVM" algorithms work well after LLSP2. Tables 4 shows that the accuracy of all classifiers was considerably improved and no classifiers failed on the preprocessed dataset. It worths to note that some classifiers perform better with specific LLSP approaches.

- LibSVM and RBF Network work better after LLSP2;

- Logistic, SMO, LazyIB1, LazyIB5, KStar, LWL, J48, J48graft and LMT work well after LLSP3.

Confusion matrices based on the above specific LLSP approaches are provided in Table 5. The structure of a confusion matrix is expressed in Section 3.2. Their precision and TPR values are provided in Table 6 as well. To evaluate the performance of corresponding classifiers with the accuracy of 100% (in Table 4) after LLSP3 their computational times are shown in Table 7. It illustrates that which classifiers will perform well after LLSP3 in terms of computational time. The performance of LMT with LLSP3 is not satisfactory since it has a long computational time (104 seconds). In conclusion, the combinations of Logistic and LazyIB1 with LLSP3 perform well for Experiment 1 with the classification accuracy of 100% and the computational time of 0.01 second.

Table 4. Classification accuracy of Experiment 1 on the test set for (a) the original dataset, 4097 features and (b) the preprocessed dataset (after LLSP1 to LLSP4), 52 features for LLSP1 and LLSP3, 101 features for LLSP2 and LLSP4.

Table 5. Confusion matrices of Experiment 1 from the prominent combinations of LLSP2 and LLSP3 with corresponding classifiers in terms of classification accuracy.

Table 6. Precision and TPR values for the prominent classifiers in combination with LLSP2 and LLSP3 for Experiment 1.

Table 7. Computational time on the test set over the preprocessed dataset after LLSP3 for Experiment 1.

Table 8 demonstrates that the accuracy of all classifiers except LibSVM considerably improved after LLSP approaches (LLSP1 to LLSP4) rather than the original dataset. Although the LibSVM classifier provides a better accuracy on the original dataset, no classification method failed on the preprocessed dataset after LLSP. Most of the classifiers in Table 8 achieved the accuracy of 100% after LLSP1. Since the maximum accuracy obtained after LLSP4 is 95% and its computational time reported in Table 2 is 4,206 seconds then, the performance of LLSP4 in Experiment 2 is not satisfactory. Moreover, the performance of LLSP2 is not satisfactory regardless of 100%

accuracy obtained from Logistic because of the long computational time (5,6104 seconds) presented in Table 2. Some classifiers in Table 8 carry out better with specific LLSP approaches.

- Logistic, J48, J48graft and LMT work well after LLSP1;
- SMO, LazyIB1, KStar and LWL perform well after LLSP1 and LLSP3;
- RBF Network and LazyIB5 work well after LLSP3.

Their confusion matrices and precision/TPR values are shown in Table 9 and 10 respectively. To investigate the performance of the corresponding classifiers after LLSP1 and LLSP3 their computational times are reported in Table 11. As discussed above, most of classifiers reached high accuracy of 100% after LLSP1 of Experiment 2. So, a preprocessing approach with polynomial amplitude (LLSP1) is preferable. Taken together, the results from Table 11 suggest that for Experiment 2 the combinations of LazyIB1 and J48 with LLSP1 perform well with the classification accuracy of 100% and zero value of computational time. The combination of LazyIB5 with LLSP3 results in the classification accuracy of 100% and the computational time of 0.01 second.

Table 8. Classification accuracy of Experiment 2 on the test set for (a) the original dataset, 4097 features and (b) the preprocessed dataset (after LLSP1 to LLSP4), 52 features for LLSP1 and LLSP3, 101 features for LLSP2 and LLSP4.

Table 9. Confusion matrices of Experiment 2 from the prominent combinations of LLSP1 and LLSP3 with corresponding classifiers in terms of classification accuracy.

Table 10. Precision and TPR values for the prominent classifiers in combination with LLSP1 and LLSP3 for Experiment 1.

Table 11. Computational time on the test set over the preprocessed dataset after LLSP1 and LLSP3 for Experiment 2.

All classifiers in Table 12 except LibSVM have achieved the better classification accuracy on the preprocessed dataset than original one. Most of the classifiers obtained the accuracy of 100% after LLSP1. The maximum

classification accuracy obtained after LLSP2 is 95% and it has a long computational time of 5,702 seconds (Table 2). Although LLSP2 is not a suitable preprocessing approach for Experiment 3, RBF Network performs well after it. LLSP4 is not a better suited method for preprocessing since it has a long computational time of 4,458 seconds (Table 2) in spite of the obtained classification accuracy of 100% for Logistic and LMT. LibSVM gives the accuracy of 55% on the original dataset and after LLSP3. So, LibSVM works better after LLSP3. There are classifiers that work perform with specific LLSP approaches as follows:

- Logistic, SMO and LMT perform well after LLSP1 and LLSP3;
- RBF Network and LWL work better after LLSP2;
- LazyIB1, LazyIB5, KStar, J48 and J48graft work well after LLSP1.

Confusion matrices and precision/TPR values of all above specific LLSPs are illustrated in Table 13 and 14 respectively. To evaluate the performance of LLSP1 and LLSP3 with the corresponding classifiers that obtained the classification accuracy of 100% the values of computational time are set out in Table 15. It is apparent from this table that the combinations of Logistic and LazyIB1 with LLSP1 and Logistic with LLSP3 perform well with the classification accuracy of 100%. Interestingly, LLSP1 is a better suited approach for Experiment 3 since most of classifiers achieved the maximum accuracy of 100% in combination with LLSP1.

Table 12. Classification accuracy of Experiment 3 on the test set for (a) the original dataset, 4097 features and (b) the preprocessed dataset (after LLSP1 to LLSP4), 52 features for LLSP1 and LLSP3, 101 features for LLSP2 and LLSP4.

Table 13. Confusion matrices of Experiment 3 from the prominent combinations of LLSP1, LLSP2 and LLSP3 with corresponding classifiers in terms of classification accuracy.

Table 14. Precision and TPR values for the prominent classifiers in combination with LLSP1, LLSP2 and LLSP3 for Experiment 3.

Table 15. Computational time on the test set after LLSP1 and LLSP3 for Experiment 3.

Table 16 presents the classification accuracy of Experiment 4 on the original and preprocessed datasets (after LLSP approaches). As it can be seen from the table below LibSVM provides a better accuracy on the original dataset rather than the preprocessed dataset. The performance of LLSP2 and LLSP4 are not satisfactory due to their long computational times for Experiment 4. The more surprising is with the simpler preprocessing approaches called LLSP1 and LLSP3. They obtained the highest classification accuracy of 100% in combination with the most of classifiers. They are faster than LLSP2 and LLSP4. In summary, some classifiers work well with specific preprocessing approaches.

- Logistic, SMO and LazyIB1, KStar, LWL and LMT perform well after LLSP1 and LLSP3;
- RBF Network and LazyIB5 work well after LLSP3;
- J48 and J48graft perform well after LLSP1.

Their confusion matrices and precision/TPR values are displayed in Table 17 and 18 respectively. To assess the performance of LLSP1 and LLSP3 in combination with the corresponding classifiers with the accuracy of 100% Table 19 is presented. Logistic and LazyIB5 perform better after LLSP1 and LLSP3 respectively while LazyIB1 performs well after both LLSP1 and LLSP3.

Table 16. Classification accuracy of Experiment 4 on the test set for (a) the original dataset, 4097 features and (b) the preprocessed dataset (after LLSP1 to LLSP4), 52 features for LLSP1 and LLSP3, 101 features for LLSP2 and LLSP4.

Table 17. Confusion matrices of Experiment 4 from the prominent combinations of LLSP1 and LLSP3 with corresponding classifiers in terms of classification accuracy.

Table 14. Precision and TPR values for the prominent classifiers in combination with LLSP1 and LLSP3 for Experiment 4.

Table 19. Computational time on the test set after LLSP1 and LLSP3 for Experiment 4.

The performance of above methods (combinations of feature extraction models and classification algorithms) based on aforementioned statistical metrics is summarized in Table 20. Therefore, no seizure segments are misclassified as non-seizure and vice versa. A comparison of classification accuracy obtained by other algorithms for epileptic seizure detection is presented in Table 21. Further, it should be noted that the total accuracy of the proposed methods in this work are improved in the case of all experiments.

Table 20. Performance of proposed methods based on corresponding statistical measures.

Table 21. Comparative performance based on the classification accuracy obtained by various methods.

4. Concluding remarks

An epileptic EEG signal has been approximated as a sine wave. Its amplitude was modelled as a polynomial of increased degree and a spline. Two new extraction models (LLSP1 and LLSP2) containing polynomial functions were developed. The parameters of each polynomial were optimised by solving a sequence of LLSPs through normal equations method if the system matrix is full-rank. An SVD is employed to solve a sequence of LLSPs if its system matrix is rank-deficient. The preprocessing approaches (LLSP1–4) are used to extract the key features of an epileptic EEG signal. Four different experiments were carried out to obtain the performance of the preprocessing models in the classification of an EEG signal. A promising performance was reported based on the evaluation criteria described in Section (3.2). The findings of this study are summarized below. Following combinations achieved the classification accuracy of 100%.

1. Logistic and LazyIB1 perform well with LLSP3 for Experiment 1;
2. LazyIB1 and J48 work well with LLSP1 and LazyIB5 performs well with LLSP3 for Experiment 2;
3. Logistic performs well with LLSP1 and LLSP3. LazyIB1 works well with LLSP1 for Experiment 3;
4. Logistic and LazyIB5 work well with LLSP1 and LLSP3 respectively and LazyIB1 performs well with both LLSP1 and LLSP3 for Experiment 4.

Generally, LLSP1 and LLSP3 are fast and accurate feature extraction methods since they are much simpler than LLSP2 and LLSP4. The best classifiers for this work were Logistic, LazyIB1, LazyIB5 and J48. The numerical results show that most of classifiers achieved the classification accuracy of 100% after LLSP1 except for Experiment 1 where LLSP3 works well. Therefore, LLSP1 carries out better in terms of classification accuracy whereas LLSP3 performs well in terms of computational time.

References

References

- [1] S. Santaniello, S. P. Burns, A. J. Golby, J. M. Singer, W. S. Anderson, S. V. Sarma, Quickest detection of drug-resistant seizures: An optimal control approach, *Epilepsy and Behavior* 22 (2011) S49–S60. doi:<http://dx.doi.org/10.1016/j.yebeh.2011.08.041>.
- [2] T. Netoff, Y. Park, K. Parhi, Seizure prediction using cost-sensitive support vector machine, in: *Engineering in Medicine and Biology Society, 2009. EMBC 2009. Annual International Conference of the IEEE, 2009*, pp. 3322–3325. doi:[10.1109/IEMBS.2009.5333711](http://dx.doi.org/10.1109/IEMBS.2009.5333711).
- [3] W. Zhou, Y. Liu, Q. Yuan, X. Li, Epileptic seizure detection using lacunarity and bayesian linear discriminant analysis in intracranial eeg, *Biomedical Engineering, IEEE Transactions on* 60 (12) (2013) 3375–3381. doi:[10.1109/TBME.2013.2254486](http://dx.doi.org/10.1109/TBME.2013.2254486).
- [4] Epilepsy Australia Ltd., *Epilepsy Australia–Information*, <http://www.epilepsyaustralia.net/epilepsy-explained/> (2014).
- [5] V. L. Dorr, M. Caparos, F. Wendling, J.-P. Vignal, D. Wolf, Extraction of reproducible seizure patterns based on EEG scalp correlations, *Biomedical Signal Processing and Control* 2 (3) (2007) 154–162. doi:<http://dx.doi.org/10.1016/j.bspc.2007.07.002>.
- [6] Y. Tang, D. Durand, A tunable support vector machine assembly classifier for epileptic seizure detection, *Expert Systems with Applications* 39 (4) (2012) 3925–3938. doi:<http://dx.doi.org/10.1016/j.eswa.2011.08.088>.
- [7] H. Adeli, Z. Zhou, N. Dadmehr, Analysis of EEG records in an epileptic patient using wavelet transform, *Journal of Neuroscience Methods* 123 (1) (2003) 69–87. doi:[http://dx.doi.org/10.1016/S0165-0270\(02\)00340-0](http://dx.doi.org/10.1016/S0165-0270(02)00340-0).
- [8] Y. Khan, J. Gotman, Wavelet based automatic seizure detection in intracerebral electroencephalogram, *Clinical Neurophysiology* 114 (5) (2003) 898–908. doi:[http://dx.doi.org/10.1016/S1388-2457\(03\)00035-X](http://dx.doi.org/10.1016/S1388-2457(03)00035-X).

- [9] S. Xie, S. Krishnan, Wavelet-based sparse functional linear model with applications to eegs se, *Medical and Biological Engineering and Computing* 51 (1–2) (2013) 49–60. doi:10.1007/s11517-012-0967-8. URL <http://dx.doi.org/10.1007/s11517-012-0967-8>
- [10] V. Srinivasan, C. Eswaran, N. Sriraam, Artificial neural network based epileptic detection using time-domain and frequency-domain, *Journal of Medical Systems* 29 (6) (2005) 647–660. doi:10.1007/s10916-005-6133-1. URL <http://dx.doi.org/10.1007/s10916-005-6133-1>
- [11] G. D. Cetin, O. Cetin, M. R. Bozkurt, Article: The detection of normal and epileptic eeg signals using ann methods with matlab-based gui, *International Journal of Computer Applications* 114 (12) (2015) 45–50.
- [12] A. Bhardwaj, A. Tiwari, R. Krishna, V. Varma, A novel genetic programming approach for epileptic seizure detection, *Computer Methods and Programs in Biomedicine* (2015) – doi:<http://dx.doi.org/10.1016/j.cmpb.2015.10.001>. URL <http://www.sciencedirect.com/science/article/pii/S016926071500262X>
- [13] R. Panda, P. Khobragade, P. Jambhule, S. Jengthe, P. Pal, T. Gandhi, Classification of eeg signal using wavelet transform and support vector machine for epileptic seizure diction, in: *Systems in Medicine and Biology (ICSMB), 2010 International Conference on*, 2010, pp. 405–408. doi:10.1109/ICSMB.2010.5735413.
- [14] S. Ghosh-Dastidar, H. Adeli, N. Dadmehr, Mixed-band wavelet-chaos-neural network methodology for epilepsy and epileptic seizure detection, *Biomedical Engineering, IEEE Transactions on* 54 (9) (2007) 1545–1551. doi:10.1109/TBME.2007.891945.
- [15] H. Ocak, Optimal classification of epileptic seizures in EEG using wavelet analysis and genetic algorithm, *Signal Processing* 88 (7) (2008) 1858–1867. doi:<http://dx.doi.org/10.1016/j.sigpro.2008.01.026>.
- [16] K. Polat, S. Gne, Classification of epileptiform EEG using a hybrid system based on decision tree classifier and fast fourier transform, *Applied Mathematics and Computation* 187 (2) (2007) 1017–1026. doi:<http://dx.doi.org/10.1016/j.amc.2006.09.022>.

- [17] R. B. Pachori, S. Patidar, Epileptic seizure classification in EEG signals using second-order di-
Computer Methods and Programs in Biomedicine 113 (2) (2014) 494–
502. doi:10.1016/j.cmpb.2013.11.014.
URL <http://dx.doi.org/10.1016/j.cmpb.2013.11.014>
- [18] V. Bajaj, R. Pachori, Classification of seizure and nonseizure EEG
signals using empirical mode decomposition, Information Technol-
ogy in Biomedicine, IEEE Transactions on 16 (6) (2012) 1135–1142.
doi:10.1109/TITB.2011.2181403.
- [19] R. G. Andrzejak, K. Lehnertz, F. Mormann, C. Rieke, P. David,
C. E. Elger, Indications of nonlinear deterministic and finite-dimensional
structures in time series of brain electrical activity: dependence on
recording region and brain state, Physical Review E. 64 (2001) 061907.
doi:10.1103/PhysRevE.64.061907.
- [20] Y. Zhang, G. Zhou, Q. Zhao, J. Jin, X. Wang, A. Cichocki, Spatial-
temporal discriminant analysis for ERP-based brain-computer interface,
Neural Systems and Rehabilitation Engineering, IEEE Transactions on
21 (2) (2013) 233–243. doi:10.1109/TNSRE.2013.2243471.
- [21] Z. R. Zamir, N. Sukhorukova, H. Amiel, A. Ugon, C. Philippe,
Optimization-based features extraction for k-complex detection, in:
M. Nelson, T. Hamilton, M. Jennings, J. Bunder (Eds.), Proceedings
of the 11th Biennial Engineering Mathematics and Applications Con-
ference, EMAC-2013, Vol. 55 of ANZIAM J., 2014, pp. C384–C398,
<http://journal.austms.org.au/ojs/index.php/ANZIAMJ/article/view/7802>
[August 27, 2014].
- [22] Z. R. Zamir, N. Sukhorukova, H. Amiel, A. Ugon, C. Philippe,
Convex optimisation-based methods for k-complex detection,
Applied Mathematics and Computation 268 (2015) 947–956.
doi:http://dx.doi.org/10.1016/j.amc.2015.07.005.
- [23] M. Hall, E. Frank, G. Holmes, B. Pfahringer, P. Reutemann, I. H.
Witten, The weka data mining software: An update, SIGKDD Explor.
Newsl. 11 (1) (2009) 10–18. doi:10.1145/1656274.1656278.
URL <http://doi.acm.org/10.1145/1656274.1656278>

- [24] Y. Zhang, G. Zhou, J. Jin, X. Wang, A. Cichocki, Frequency recognition in SSVEP-based BCI using multiset canonical correlation analysis, *International Journal of Neural Systems* 24 (04) (2014) 1450013, pMID: 24694168. arXiv:<http://www.worldscientific.com/doi/pdf/10.1142/S0129065714500130>, doi:10.1142/S0129065714500130. URL <http://www.worldscientific.com/doi/abs/10.1142/S0129065714500130>
- [25] Z. R. Zamir, N. Sukhorukova, Linear least squares problems involving fixed knots polynomial. *Applied Mathematics and Computation* 282 (2016) 204–215. doi:<http://dx.doi.org/10.1016/j.amc.2016.02.011>. URL <http://www.sciencedirect.com/science/article/pii/S009630031630114X>
- [26] D. Moloney, N. Sukhorukova, P. Vamplew, J. Ugon, G. Li, G. Beliakov, C. Philippe, H. Amiel, A. Ugon, Detecting k-complexes for sleep stage identification using nonsmooth optimization, *The ANZIAM Journal* 52 (2011) 319–332.
- [27] M. J. D. Powell, Curve fitting by cubic splines, Rep. TP 307, Atomic Energy Res. Est., Harwell, England, 1967.
- [28] J. R. Rice, *The approximation of functions*, Vol. II, Addison-Wesley, Reading, Massachusetts, 1969.
- [29] S. Wold, Spline functions in data analysis, *Technometrics* 16 (1) (1974) pp. 1–11. URL <http://www.jstor.org/stable/1267485>
- [30] G. Nürnberger, *Approximation by Spline Functions*, Springer-Verlag, Berlin Heidelberg, 1989. URL <http://books.google.com.au/books?id=-0F4QgAACAAJ>
- [31] V. F. Dem'janov, V. N. Malozemov, D. Louvish, *Introduction to Minimax*, Wiley, 1974. URL <https://books.google.com.au/books?id=sag3nwEACAAJ>
- [32] N. G. Chebotarev, On a certain minimax criterion, *Dokl. Akad. Nauk SSSR* 39, 373–376 (see also *Collected Works Vol. 2*, Moscow, Izdatel'stvo Akad, Nauk SSSR, 1949), 1943.

- [33] A. Björck, Numerical Methods for Least Squares Problems, Handbook of Numerical Analysis, Society for Industrial and Applied Mathematics, 1996.
- [34] J. L. Barlow, Numerical aspects of solving linear least squares problems, Tech. rep., Computer Science Department, The Pennsylvania State University, University Park, PA, USA (January 1999).
- [35] S. Boyd, L. Vandenberghe, Convex Optimization, Cambridge University Press, New York, NY, USA, 2010.
- [36] L. N. Trefethen, D. Bau, Numerical Linear Algebra, Miscellaneous Bks, Cambridge University Press, 1997.
- [37] A. T. Tzallas, M. G. Tsipouras, D. I. Fotiadis, Automatic seizure detection based on time-frequency analysis and artificial neural networks, Computational Intelligence and Neuroscience 2007 (2007) 80510. doi:10.1155/2007/80510. URL <http://www.ncbi.nlm.nih.gov/pmc/articles/PMC2246039/>
- [38] L. Guo, D. Rivero, A. Pazos, Epileptic seizure detection using multiwavelet transform based approximate entropy and artificial neural networks, Journal of Neuroscience Methods 193 (1) (2010) 156–163. doi:<http://dx.doi.org/10.1016/j.jneumeth.2010.08.030>.
- [39] S. Dehuri, A. K. Jagadev, S.-B. Cho, Epileptic seizure identification from electroencephalography signal using DE-RBFNs ensemble, Procedia Computer Science 23 (2013) 84–95, 4th International Conference on Computational Systems-Biology and Bioinformatics, CSBio2013. doi:<http://dx.doi.org/10.1016/j.procs.2013.10.012>.
- [40] H. Ocak, Automatic detection of epileptic seizures in EEG using discrete wavelet transform and approximate entropy, Expert Systems with Applications 36 (2, Part 1) (2009) 2027–2036. doi:<http://dx.doi.org/10.1016/j.eswa.2007.12.065>.
- [41] L. Guo, D. Rivero, J. Dorado, J. R. Rabual, A. Pazos, Automatic epileptic seizure detection in EEGs based on line length feature and artificial neural networks, Journal of Neuroscience Methods 191 (1) (2010) 101–109. doi:<http://dx.doi.org/10.1016/j.jneumeth.2010.05.020>.

- [42] A. Tzallas, M. Tsipouras, D. Fotiadis, Epileptic seizure detection in EEGs using time frequency analysis, *Information Technology in Biomedicine, IEEE Transactions on* 13 (5) (2009) 703–710. doi:10.1109/TITB.2009.2017939.
- [43] S.-F. Liang, H.-C. Wang, W.-L. Chang, Combination of EEG complexity and spectral analysis for epilepsy diagnosis and seizure detection, *EURASIP J. Adv. Signal Process* 2010 (2010) 62:1–62:15. URL <http://dx.doi.org/10.1155/2010/853434>
- [44] Y. Song, P. Lio, A new approach for epileptic seizure detection: sample entropy based feature extraction, *Journal of Biomedical Science and Engineering* 3 (6) (2010) 556–567. doi:10.4236/jbise.2010.36078. URL <http://www.SciRP.org/journal/jbise/>
- [45] D. K. Ravish, S. Shenbaga Devi, S. G. Krishnamoorthy, M. R. Karthikeyan, Detection of epileptic seizure in EEG recordings by spectral method and statistical analysis, *Journal of Applied Sciences* 13 (2) (2013) 207–219. doi:10.3923/jas.2013.207.219. URL <http://scialert.net/abstract/?doi=jas.2013.207.219>
- [46] D. Nigam, V. P. and Graupe, A neural-network-based detection of epilepsy, *Neurological research* 26 (1) (2004) 55–60. doi:10.1179/016164104773026534.
- [47] V. Srinivasan, C. Eswaran, N. Sriraam, Artificial neural network based epileptic detection using time-domain and frequency-domain features, *Journal of Medical Systems* 29 (6) (2005) 647–660. doi:10.1007/s10916-005-6133-1. URL <http://dx.doi.org/10.1007/s10916-005-6133-1>
- [48] N. Kannathal, M. L. Choo, U. R. Acharya, P. Sadasivan, Entropies for detection of epilepsy in EEG, *Computer Methods and Programs in Biomedicine* 80 (3) (2005) 187–194. doi:<http://dx.doi.org/10.1016/j.cmpb.2005.06.012>.
- [49] N. Kannathal, U. R. Acharya, C. M. Lim, P. K. Sadasivan, Characterization of EEG a comparative study.

- [50] A. Subasi, EEG signal classification using wavelet feature extraction and a mixture of expert model, *Expert Systems with Applications* 32 (4) (2007) 1084–1093. doi:<http://dx.doi.org/10.1016/j.eswa.2006.02.005>.
- [51] L. Guo, D. Rivero, J. A. Seoane, A. Pazos, Classification of eeg signals using relative wavelet energy and artificial neural networks, in: *Proceedings of the First ACM/SIGEVO Summit on Genetic and Evolutionary Computation, GEC '09*, ACM, New York, NY, USA, 2009, pp. 177–184. URL <http://doi.acm.org/10.1145/1543834.1543860>
- [52] G. D. Cetin, O. Cetin, M. R. Bozkurt, The detection of normal and epileptic EEG signals using ANN methods with matlab-based gui, *International Journal of Computer Applications* 114 (12) (2015) 45–50. doi:10.5120/20034-2145.

Captions of Figure

Figure 1 : LLSP approaches Flowchart.

Figure 2 : Approximation curve after LLSP3.

Figure 3 : Segments selection of Experiment 1 for datasets balancing.

Figure 4 : Segments selection of Experiment 2 for datasets balancing.

Captions of Tables

Table 1 : Description of the datasets belongs to the experiments.

Table 2 : Computational time (in seconds) for preprocessing.

Table 3 : Mean frequencies for each set of the EEG signal.

Table 4 : Classification accuracy of Experiment 1 on the test set for (a) the original dataset, 4097 features and (b) the preprocessed dataset (after LLSP1 to LLSP4), 52 features for LLSP1 and LLSP3, 101 features for LLSP2 and LLSP4.

Table 5 : Confusion matrices of Experiment 1 from the prominent combinations of LLSP2 and LLSP3 with corresponding classifiers in terms of classification accuracy.

Table 6 : Precision and TPR values for the prominent classifiers in combination with LLSP2 and LLSP3 for Experiment 1.

Table 7 : Computational time on the test set over the preprocessed dataset after LLSP3 for Experiment 1.

Table 8 : Classification accuracy of Experiment 2 on the test set for (a) the original dataset, 4097 features and (b) the preprocessed dataset (after LLSP1 to LLSP4), 52 features for LLSP1 and LLSP3, 101 features for LLSP2 and LLSP4.

Table 9 : Confusion matrices of Experiment 2 from the prominent combinations of LLSP1 and LLSP3 with corresponding classifiers in terms of classification accuracy.

- Table 10 : Precision and TPR values for the prominent classifiers in combination with LLSP1 and LLSP3 for Experiment 2.
- Table 11 : Computational time on the test set over the preprocessed dataset after LLSP1 and LLSP3 for Experiment 2.
- Table 12 : Classification accuracy of Experiment 3 on the test set for (a) the original dataset, 4097 features and (b) the preprocessed dataset (after LLSP1 to LLSP4), 52 features for LLSP1 and LLSP3, 101 features for LLSP2 and LLSP4.
- Table 13 : Confusion matrices of Experiment 3 from the prominent combinations of LLSP1, LLSP2 and LLSP3 with corresponding classifiers in terms of classification accuracy.
- Table 14 : Precision and TPR values for the prominent classifiers in combination with LLSP1, LLSP2 and LLSP3 for Experiment 3.
- Table 15 : Computational time on the test set after LLSP1 and LLSP3 for Experiment 3.
- Table 16 : Classification accuracy of Experiment 4 on the test set for (a) the original dataset, 4097 features and (b) the preprocessed dataset (after LLSP1 to LLSP4), 52 features for LLSP1 and LLSP3, 101 features for LLSP2 and LLSP4.
- Table 17 : Confusion matrices of Experiment 4 from the prominent combinations of LLSP1 and LLSP3 with corresponding classifiers in terms of classification accuracy.
- Table 14 : Precision and TPR values for the prominent classifiers in combination with LLSP1 and LLSP3 for Experiment 4.
- Table 19 : Computational time on the test set after LLSP1 and LLSP3 for Experiment 4.
- Table 20 : Performance of proposed methods based on corresponding statistical measures.
- Table 21 : Comparative performance based on the classification accuracy obtained by various methods.

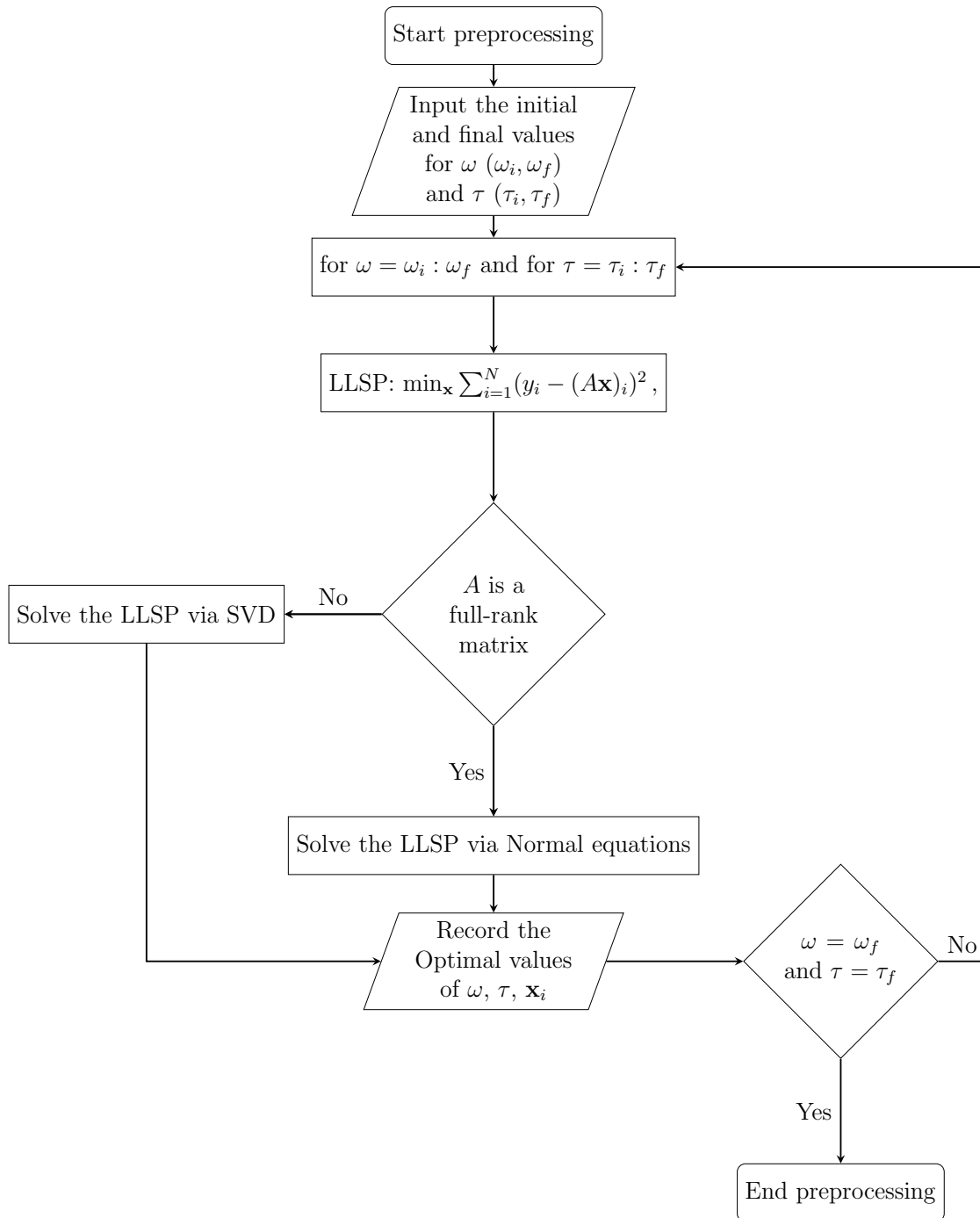


Figure 1: LLSP approaches Flowchart

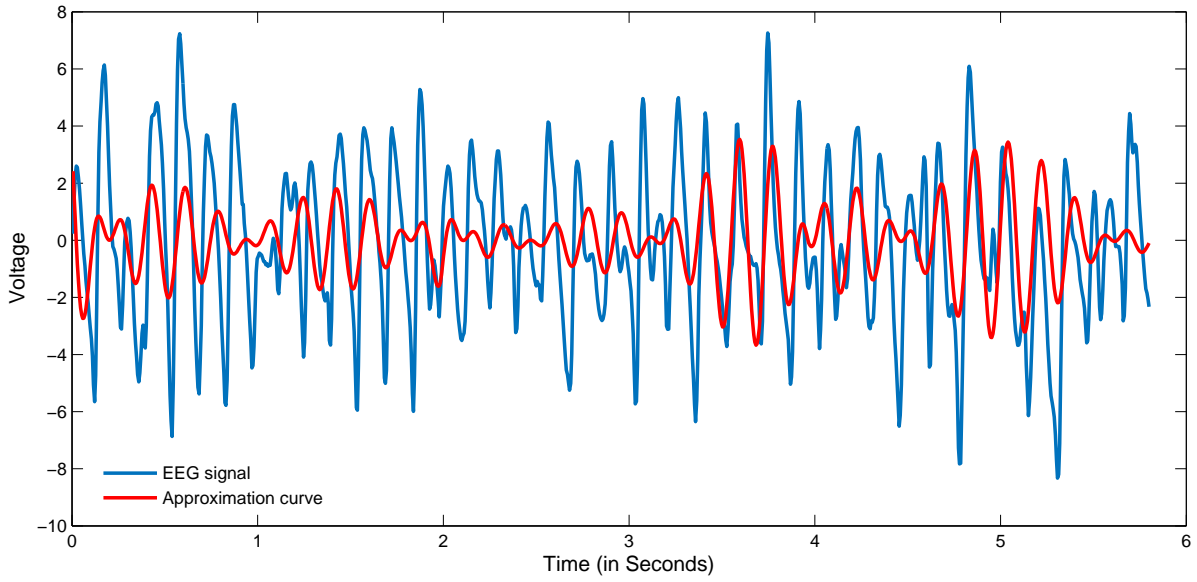


Figure 2: Approximation curve after LLSP3.

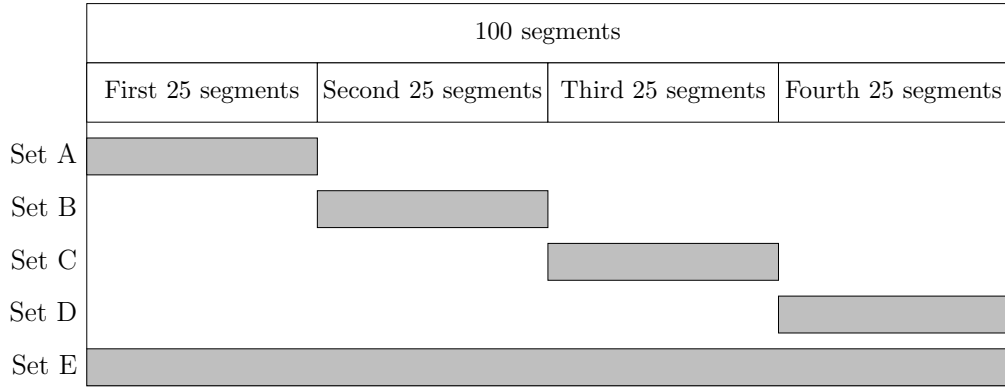


Figure 3: Segments selection of Experiment 1 for datasets balancing.

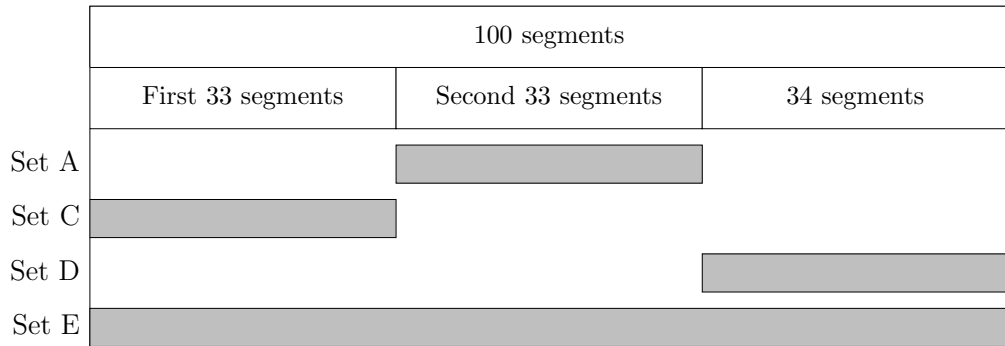


Figure 4: Segments selection of Experiment 2 for datasets balancing.

Table 1: Description of the datasets belongs to the experiments.

Experiment #	Classes		Segments		Total Channels
	Non-seizure	Seizure	Non-seizure	Seizure	
1 (ABCD-E)	ABCD	E	100	100	200
2 (ACD-E)	ACD	E	100	100	200
3 (B-E)	B	E	100	100	200
4 (A-E)	A	E	100	100	200

Table 2: Computational time (in seconds) for preprocessing.

LLSP approaches	LLSP1	LLSP2	LLSP3	LLSP4
Experiment 1	2,209	5,652	1,562	4,219
Experiment 2	2,190	5,610	1,774	4,206
Experiment 3	2,223	5,702	1,723	4,458
Experiment 4	2,184	5,631	1,597	4,456

Table 3: Mean frequencies for each set of the EEG signal.

LLSP approaches	LLSP1	LLSP2	LLSP3	LLSP4
Set A	0.7500	1.9900	0.5400	1.9500
Set B	6.5800	6.9600	5.2500	9.6600
Set C	0.9800	1.4300	0.8000	1.1800
Set D	1.6800	1.7883	1.3300	1.9700
Set E	5.1100	5.0600	4.8500	4.9100

Table 4: Classification accuracy of Experiment 1 on the test set for (a) the original dataset, 4097 features and (b) the preprocessed dataset (after LLSP1 to LLSP4), 52 features for LLSP1 and LLSP3, 101 features for LLSP2 and LLSP4.

Accuracy on (a)	Accuracy on (b)				Classifiers
	LLSP1	LLSP2	LLSP3	LLSP4	
45%	45%	50%	45%	45%	LibSVM
N/A ^a	95%	91%	100%	95%	Logistic
54%	68%	86%	68%	45%	RBF Network
N/A ^a	77%	91%	100%	95%	SMO
64%	77%	82%	100%	86%	LazyIB1
68%	73%	77%	91%	91%	LazyIB5
54%	82%	86%	100%	55%	KStar
68%	77%	86%	100%	86%	LWL
54%	55%	55%	55%	55%	OneR
45%	82%	91%	100%	95%	J48
45%	82%	91%	100%	95%	J48graft
N/A ^a	82%	91%	100%	91%	LMT

^a No Answer.

Table 5: Confusion matrices of Experiment 1 from the prominent combinations of LLSP2 and LLSP3 with corresponding classifiers in terms of classification accuracy.

Original dataset	Preprocessed dataset		Classifiers
	LLSP2	LLSP3	
$\begin{pmatrix} 0 & 12 \\ 0 & 10 \end{pmatrix}$	$\begin{pmatrix} 1 & 11 \\ 0 & 10 \end{pmatrix}$		LibSVM
N/A ^a		$\begin{pmatrix} 12 & 0 \\ 0 & 10 \end{pmatrix}$	Logistic
$\begin{pmatrix} 12 & 0 \\ 10 & 0 \end{pmatrix}$	$\begin{pmatrix} 11 & 1 \\ 2 & 8 \end{pmatrix}$		RBF Network
N/A ^a		$\begin{pmatrix} 12 & 0 \\ 0 & 10 \end{pmatrix}$	SMO
$\begin{pmatrix} 12 & 0 \\ 8 & 2 \end{pmatrix}$		$\begin{pmatrix} 12 & 0 \\ 0 & 10 \end{pmatrix}$	LazyIB1
$\begin{pmatrix} 12 & 0 \\ 7 & 3 \end{pmatrix}$		$\begin{pmatrix} 12 & 0 \\ 2 & 8 \end{pmatrix}$	LazyIB5
$\begin{pmatrix} 12 & 0 \\ 10 & 0 \end{pmatrix}$		$\begin{pmatrix} 12 & 0 \\ 0 & 10 \end{pmatrix}$	KStar
$\begin{pmatrix} 12 & 0 \\ 7 & 3 \end{pmatrix}$		$\begin{pmatrix} 12 & 0 \\ 0 & 10 \end{pmatrix}$	LWL
$\begin{pmatrix} 0 & 12 \\ 0 & 10 \end{pmatrix}$		$\begin{pmatrix} 12 & 0 \\ 0 & 10 \end{pmatrix}$	J48
$\begin{pmatrix} 0 & 12 \\ 0 & 10 \end{pmatrix}$		$\begin{pmatrix} 12 & 0 \\ 0 & 10 \end{pmatrix}$	J48graft
N/A ^a		$\begin{pmatrix} 12 & 0 \\ 0 & 10 \end{pmatrix}$	LMT

^a No Answer.

Table 6: Precision and TPR values for the prominent classifiers in combination with LLSP2 and LLSP3 for Experiment 1.

Precision/TPR Original dataset	Precision/TPR		Classifiers
	LLSP2	LLSP3	
N/A ^a / 0	1.00 / 0.08		LibSVM
N/A ^a		1.00 / 1.00	Logistic
0.55 / 1.00	0.85 / 0.92		RBF Network
N/A ^a		1.00 / 1.00	SMO
0.60 / 1.00		1.00 / 1.00	LazyIB1
0.63 / 1.00		0.86 / 1.00	LazyIB5
0.55 / 1.00		1.00 / 1.00	KStar
0.63 / 1.00		1.00 / 1.00	LWL
N/A ^a / 0		1.00 / 1.00	J48
N/A ^a / 0		1.00 / 1.00	J48graft
N/A ^a		1.00 / 1.00	LMT

^a No Answer.

Table 7: Computational time on the test set over the preprocessed dataset after LLSP3 for Experiment 1.

Classifiers	CPU time (in seconds)
Logistic	0.01
SMO	0.17
LazyIB1	0.01
KStar	0.05
LWL	0.06
J48	0.02
J48graft	0.18
LMT	104

Table 8: Classification accuracy of Experiment 2 on the test set for (a) the original dataset, 4097 features and (b) the preprocessed dataset (after LLSP1 to LLSP4), 52 features for LLSP1 and LLSP3, 101 features for LLSP2 and LLSP4.

Accuracy on (a)	Accuracy on (b)				Classifiers
	LLSP1	LLSP2	LLSP3	LLSP4	
85%	50%	55%	60%	50%	LibSVM
N/A ^a	100%	100%	95%	95%	Logistic
50%	85%	75%	90%	50%	RBF Network
N/A ^a	100%	85%	100%	95%	SMO
65%	100%	80%	100%	80%	LazyIB1
65%	95%	70%	100%	85%	LazyIB5
50%	100%	80%	100%	50%	KStar
65%	100%	90%	100%	95%	LWL
50%	50%	50%	50%	50%	OneR
50%	100%	95%	95%	95%	J48
50%	100%	95%	95%	95%	J48graft
N/A ^a	100%	85%	95%	91%	LMT

^a No Answer.

Table 9: Confusion matrices of Experiment 2 from the prominent combinations of LLSP1 and LLSP3 with corresponding classifiers in terms of classification accuracy.

Original dataset	Preprocessed dataset		Classifiers
	LLSP1	LLSP3	
N/A ^a	$\begin{pmatrix} 10 & 0 \\ 0 & 10 \end{pmatrix}$		Logistic
$\begin{pmatrix} 10 & 0 \\ 10 & 0 \end{pmatrix}$		$\begin{pmatrix} 9 & 1 \\ 1 & 9 \end{pmatrix}$	RBF Network
N/A ^a	$\begin{pmatrix} 10 & 0 \\ 0 & 10 \end{pmatrix}$	$\begin{pmatrix} 10 & 0 \\ 0 & 10 \end{pmatrix}$	SMO
$\begin{pmatrix} 10 & 0 \\ 7 & 3 \end{pmatrix}$	$\begin{pmatrix} 10 & 0 \\ 0 & 10 \end{pmatrix}$	$\begin{pmatrix} 10 & 0 \\ 0 & 10 \end{pmatrix}$	LazyIB1
$\begin{pmatrix} 10 & 0 \\ 7 & 3 \end{pmatrix}$		$\begin{pmatrix} 10 & 0 \\ 0 & 10 \end{pmatrix}$	LazyIB5
$\begin{pmatrix} 10 & 0 \\ 10 & 0 \end{pmatrix}$	$\begin{pmatrix} 10 & 0 \\ 0 & 10 \end{pmatrix}$	$\begin{pmatrix} 10 & 0 \\ 0 & 10 \end{pmatrix}$	KStar
$\begin{pmatrix} 10 & 0 \\ 7 & 3 \end{pmatrix}$	$\begin{pmatrix} 10 & 0 \\ 0 & 10 \end{pmatrix}$	$\begin{pmatrix} 10 & 0 \\ 0 & 10 \end{pmatrix}$	LWL
$\begin{pmatrix} 10 & 0 \\ 10 & 0 \end{pmatrix}$	$\begin{pmatrix} 10 & 0 \\ 0 & 10 \end{pmatrix}$		J48
$\begin{pmatrix} 10 & 0 \\ 10 & 0 \end{pmatrix}$	$\begin{pmatrix} 10 & 0 \\ 0 & 10 \end{pmatrix}$		J48graft
N/A ^a	$\begin{pmatrix} 10 & 0 \\ 0 & 10 \end{pmatrix}$		LMT

^a No Answer.

Table 10: Precision and TPR values for the prominent classifiers in combination with LLSP1 and LLSP3 for Experiment 2.

Precision/TPR	Precision/TPR		Classifiers
Original dataset	LLSP1	LLSP3	
N/A ^a	1.00 / 1.00		Logistic
0.50 / 1.00		0.90 / 0.90	RBF Network
N/A ^a	1.00 / 1.00	1.00 / 1.00	SMO
0.60 / 1.00	1.00 / 1.00	1.00 / 1.00	LazyIB1
0.60 / 1.00		1.00 / 1.00	LazyIB5
0.50 / 1.00	1.00 / 1.00	1.00 / 1.00	KStar
0.60 / 1.00	1.00 / 1.00	1.00 / 1.00	LWL
0.50 / 1.00	1.00 / 1.00		J48
0.50 / 1.00	1.00 / 1.00		J48graft
N/A ^a	1.00 / 1.00		LMT

^a No Answer.

Table 11: Computational time on the test set over the preprocessed dataset after LLSP1 and LLSP3 for Experiment 2.

Classifiers with LLSP1	CPU time (in seconds)
Logistic	0.03
SMO	0.22
LazyIB1	0
KStar	0.05
LWL	0.05
J48	0
J48graft	0.12
LMT	89
Classifiers with LLSP3	CPU time (in seconds)
SMO	0.15
LazyIB1	0.01
LazyIB5	0.01
KStar	0.13
LWL	0.16

Table 12: Classification accuracy of Experiment 3 on the test set for (a) the original dataset, 4097 features and (b) the preprocessed dataset (after LLSP1 to LLSP4), 52 features for LLSP1 and LLSP3, 101 features for LLSP2 and LLSP4.

Accuracy on (a)	Accuracy on (b)				Classifiers
	LLSP1	LLSP2	LLSP3	LLSP4	
55%	50%	50%	55%	50%	LibSVM
N/A ^a	100%	95%	100%	100%	Logistic
50%	50%	90%	65%	70%	RBF Network
N/A ^a	100%	95%	100%	95%	SMO
65%	100%	95%	90%	95%	LazyIB1
60%	95%	85%	90%	95%	LazyIB5
50%	100%	95%	90%	50%	KStar
65%	90%	95%	80%	95%	LWL
50%	50%	50%	50%	50%	OneR
50%	100%	95%	95%	95%	J48
50%	100%	95%	95%	95%	J48graft
N/A ^a	100%	95%	100%	100%	LMT

^a No Answer.

Table 13: Confusion matrices of Experiment 3 from the prominent combinations of LLSP1, LLSP2 and LLSP3 with corresponding classifiers in terms of classification accuracy.

Original dataset	Preprocessed dataset			Classifiers
	LLSP1	LLSP2	LLSP3	
N/A ^a	$\begin{pmatrix} 10 & 0 \\ 0 & 10 \end{pmatrix}$		$\begin{pmatrix} 10 & 0 \\ 0 & 10 \end{pmatrix}$	Logistic
$\begin{pmatrix} 10 & 0 \\ 10 & 0 \end{pmatrix}$		$\begin{pmatrix} 10 & 0 \\ 2 & 8 \end{pmatrix}$		RBF Network
N/A ^a	$\begin{pmatrix} 10 & 0 \\ 0 & 10 \end{pmatrix}$		$\begin{pmatrix} 10 & 0 \\ 0 & 10 \end{pmatrix}$	SMO
$\begin{pmatrix} 10 & 0 \\ 7 & 3 \end{pmatrix}$	$\begin{pmatrix} 10 & 0 \\ 0 & 10 \end{pmatrix}$			LazyIB1
$\begin{pmatrix} 10 & 0 \\ 8 & 2 \end{pmatrix}$	$\begin{pmatrix} 10 & 0 \\ 1 & 9 \end{pmatrix}$			LazyIB5
$\begin{pmatrix} 10 & 0 \\ 10 & 0 \end{pmatrix}$	$\begin{pmatrix} 10 & 0 \\ 0 & 10 \end{pmatrix}$			KStar
$\begin{pmatrix} 10 & 0 \\ 7 & 3 \end{pmatrix}$		$\begin{pmatrix} 10 & 0 \\ 1 & 9 \end{pmatrix}$		LWL
$\begin{pmatrix} 10 & 0 \\ 10 & 0 \end{pmatrix}$	$\begin{pmatrix} 10 & 0 \\ 0 & 10 \end{pmatrix}$			J48
$\begin{pmatrix} 10 & 0 \\ 10 & 0 \end{pmatrix}$	$\begin{pmatrix} 10 & 0 \\ 0 & 10 \end{pmatrix}$			J48graft
N/A ^a	$\begin{pmatrix} 10 & 0 \\ 0 & 10 \end{pmatrix}$		$\begin{pmatrix} 10 & 0 \\ 0 & 10 \end{pmatrix}$	LMT

^a No Answer.

Table 14: Precision and TPR values for the prominent classifiers in combination with LLSP1, LLSP2 and LLSP3 for Experiment 3.

Precision/TPR	Precision/TPR			Classifiers
Original dataset	LLSP1	LLSP2	LLSP3	
N/A ^a	1.00 / 1.00		1.00 / 1.00	Logistic
0.50 / 1.00		0.83 / 1.00		RBF Network
N/A ^a	1.00 / 1.00		1.00 / 1.00	SMO
0.59 / 1.00	1.00 / 1.00			LazyIB1
0.55 / 1.00	0.91 / 1.00			LazyIB5
0.50 / 1.00	1.00 / 1.00			KStar
0.59 / 1.00		0.91 / 1.00		LWL
0.50 / 1.00	1.00 / 1.00			J48
0.50 / 1.00	1.00 / 1.00			J48graft
N/A ^a	1.00 / 1.00		1.00 / 1.00	LMT

^a No Answer.

Table 15: Computational time on the test set after LLSP1 and LLSP3 for Experiment 3.

Classifiers with LLSP1	CPU time (in seconds)
Logistic	0.01
SMO	0.12
LazyIB1	0.01
KStar	0.05
J48	0.02
J48graft	0.45
LMT	124
Classifiers with LLSP3	CPU time (in seconds)
Logistic	0.01
SMO	0.15
LMT	138

Table 16: Classification accuracy of Experiment 4 on the test set for (a) the original dataset, 4097 features and (b) the preprocessed dataset (after LLSP1 to LLSP4), 52 features for LLSP1 and LLSP3, 101 features for LLSP2 and LLSP4.

Accuracy on (a)	Accuracy on (b)				Classifiers
	LLSP1	LLSP2	LLSP3	LLSP4	
75%	50%	55%	65%	55%	LibSVM
N/A ^a	100%	90%	100%	90%	Logistic
50%	50%	85%	85%	50%	RBF Network
N/A ^a	100%	90%	100%	95%	SMO
65%	100%	85%	100%	85%	LazyIB1
65%	95%	85%	100%	80%	LazyIB5
50%	100%	85%	100%	50%	KStar
65%	100%	80%	100%	95%	LWL
55%	50%	50%	50%	50%	OneR
50%	100%	90%	95%	90%	J48
50%	100%	90%	95%	90%	J48graft
N/A ^a	100%	90%	100%	95%	LMT

^a No Answer.

Table 17: Confusion matrices of Experiment 4 from the prominent combinations of LLSP1 and LLSP3 with corresponding classifiers in terms of classification accuracy.

Original dataset	Preprocessed dataset		Classifiers
	LLSP1	LLSP3	
N/A ^a	$\begin{pmatrix} 10 & 0 \\ 0 & 10 \end{pmatrix}$	$\begin{pmatrix} 10 & 0 \\ 0 & 10 \end{pmatrix}$	Logistic
$\begin{pmatrix} 10 & 0 \\ 10 & 0 \end{pmatrix}$		$\begin{pmatrix} 7 & 3 \\ 0 & 10 \end{pmatrix}$	RBF Network
N/A ^a	$\begin{pmatrix} 10 & 0 \\ 0 & 10 \end{pmatrix}$	$\begin{pmatrix} 10 & 0 \\ 0 & 10 \end{pmatrix}$	SMO
$\begin{pmatrix} 10 & 0 \\ 7 & 3 \end{pmatrix}$	$\begin{pmatrix} 10 & 0 \\ 0 & 10 \end{pmatrix}$	$\begin{pmatrix} 10 & 0 \\ 0 & 10 \end{pmatrix}$	LazyIB1
$\begin{pmatrix} 10 & 0 \\ 7 & 3 \end{pmatrix}$		$\begin{pmatrix} 10 & 0 \\ 0 & 10 \end{pmatrix}$	LazyIB5
$\begin{pmatrix} 10 & 0 \\ 10 & 0 \end{pmatrix}$	$\begin{pmatrix} 10 & 0 \\ 0 & 10 \end{pmatrix}$	$\begin{pmatrix} 10 & 0 \\ 0 & 10 \end{pmatrix}$	KStar
$\begin{pmatrix} 10 & 0 \\ 7 & 3 \end{pmatrix}$	$\begin{pmatrix} 10 & 0 \\ 0 & 10 \end{pmatrix}$	$\begin{pmatrix} 10 & 0 \\ 0 & 10 \end{pmatrix}$	LWL
$\begin{pmatrix} 10 & 0 \\ 10 & 0 \end{pmatrix}$	$\begin{pmatrix} 10 & 0 \\ 0 & 10 \end{pmatrix}$		J48
$\begin{pmatrix} 10 & 0 \\ 10 & 0 \end{pmatrix}$	$\begin{pmatrix} 10 & 0 \\ 0 & 10 \end{pmatrix}$		J48graft
N/A ^a	$\begin{pmatrix} 10 & 0 \\ 0 & 10 \end{pmatrix}$	$\begin{pmatrix} 10 & 0 \\ 0 & 10 \end{pmatrix}$	LMT

^a No Answer.

Table 18: Precision and TPR values for the prominent classifiers in combination with LLSP1 and LLSP3 for Experiment 4.

Precision/TPR Original dataset	Precision/TPR		Classifiers
	LLSP1	LLSP3	
N/A ^a	1.00 / 1.00	1.00 / 1.00	Logistic
0.50 / 1		0.89 / 0.80	RBF Network
N/A ^a	1.00 / 1.00	1.00 / 1.00	SMO
0.59 / 1.00	1.00 / 1.00	1.00 / 1.00	LazyIB1
0.59 / 1.00		1.00 / 1.00	LazyIB5
0.50 / 1.00	1.00 / 1.00	1.00 / 1.00	KStar
0.59 / 1.00	1.00 / 1.00	1.00 / 1.00	LWL
0.50 / 1.00	1.00 / 1.00		J48
0.50 / 1.00	1.00 / 1.00		J48graft
N/A ^a	1.00 / 1.00	1.00 / 1.00	LMT

^a No Answer.

Table 19: Computational time on the test set after LLSP1 and LLSP3 for Experiment 4.

Classifiers with LLSP1	CPU time (in seconds)
Logistic	0.01
SMO	0.14
LazyIB1	0.01
KStar	0.07
LWL	0.06
J48	0.02
J48graft	0.34
LMT	90
Classifiers with LLSP3	CPU time (in seconds)
Logistic	0.03
SMO	0.13
LazyIB1	0.01
LazyIB5	0.01
KStar	0.05
LWL	0.15
LMT	96

h

Table 20: Performance of proposed methods based on corresponding statistical measures.

Method	Experiment	TPR	TNR	FPR	FNR
LLSP3+Logistic, LazyIB1	1	1	1	0	0
LLSP1+LazyIB1, J48	2	1	1	0	0
LLSP3+LazyIB5	2	1	1	0	0
LLSP1+Logistic, LazyIB1	3	1	1	0	0
LLSP3+Logistic	3	1	1	0	0
LLSP1+Logistic, LazyIB1	4	1	1	0	0
LLSP3+LazyIB1, LazyIB5	4	1	1	0	0

Table 21: Comparative performance based on the classification accuracy obtained by various methods.

Method	Experiment	ACC (%)
Time frequency analysis-artificial neuralnetwork [37]	1	97.73
Multi-wavelet transform and approximate entropy feature-MLPNN [38]	1	98.27
Wavelet-based sparse functional linear model [9]	1	100
DE-RBFNs ensemble [39]	1	97.60
LLSP3-Logistic, LazyIB1 (this work)	1	100
DE-RBFNs ensemble [39]	2	99.25
Discrete wavelet transform-approximate entropy (ApEn) [40]	2	96.65
Discrete wavelet transform-line length feature-MLPNN [41]	2	97.75
LLSP1-LazyIB1, J48 (this work)	2	100
Time frequency analysis [42]	3	94.50
EEG complexity and spectral analysis [43]	3	98.33
Sample entropy and extreme learning machine [44]	3	95.67
Spectral method and statistical analysis [45]	3	97.50
LLSP1-Logistic, LazyIB1 (this work)	3	100
LLSP3-Logistic (this work)	3	100
Nonlinear pre-processing filter-Diagnostic neural network [46]	4	97.2
Time frequency domain features-Recurrent neural network [47]	4	99.6
Entropy measures-Adaptive neuro-fuzzy inference system [48]	4	92.22
Chaotic measures-Surrogate data analysis [49]	4	90
Fast Fourier transform-Decision tree [16]	4	98.72
Discrete wavelet transform-Mixture of expert model [50]	4	95
Time frequency analysis-Artificial neural network [37]	4	100
Discrete wavelet transform-relative wavelet energy-MLPNN [51]	4	95.2
Discrete wavelet transform-line length feature-MLPNN [41]	4	99.6
ANN methods [52]	4	98.3
LLSP1-Logistic, LazyIB1 (this work)	4	100
LLSP3-LazyIB1, LazyIB5 (this work)	4	100

